

H. M. Yin

G. H. Paulino¹
e-mail: paulino@uiuc.edu

W. G. Buttlar

Department of Civil and Environmental
Engineering,
Newmark Laboratory,
University of Illinois at Urbana-Champaign,
205 North Mathews Avenue,
Urbana, IL 61801

L. Z. Sun

Department of Civil and Environmental
Engineering,
University of California,
4139 Engineering Gateway,
Irvine, CA 92697

Effective Thermal Conductivity of Functionally Graded Particulate Nanocomposites With Interfacial Thermal Resistance

By means of a fundamental solution for a single inhomogeneity embedded in a functionally graded material matrix, a self-consistent model is proposed to investigate the effective thermal conductivity distribution in a functionally graded particulate nanocomposite. The “Kapitza thermal resistance” along the interface between a particle and the matrix is simulated with a perfect interface but a lower thermal conductivity of the particle. The results indicate that the effective thermal conductivity distribution greatly depends on Kapitza thermal resistance, particle size, and degree of material gradient.

[DOI: 10.1115/1.2936893]

Keywords: functionally graded nanocomposites, effective thermal conductivity, self-consistent method, Kapitza thermal resistance, heat conduction

1 Introduction

Functionally graded materials (FGMs) are characterized by spatially varied microstructures of constituent phases and gradual variation of effective material properties. This class of materials has received considerable attention from researchers and engineers because of their unique and attractive thermomechanical properties [1–8]. Especially noteworthy in the area of mechanics of FGMs is the contribution of Erdogan and co-workers—see, for example, Refs. [1,4]. With miniaturization of microelectronic elements and coating components, FGMs with embedded nanoparticles (nano-FGMs) can be utilized in very small, lightweight components, while retaining the excellent physical properties of nanomaterials [9,10]. For instance, Zhang et al. [11] proposed to use nano-FGMs to construct a coupling solar energy generator system maximally utilizing both photo- and thermoelectric energies. However, with the decrease of particle size in an FGM, the surface-to-volume ratio of particles increases, such that the interface between a particle and the surrounding matrix produces a considerable effect on the effective material behavior, especially in the case of nano-FGMs.

In 1941, Kapitza [12] presented measurements indicating the existence of a temperature discontinuity near the interface between helium and a solid in the presence of a heat flux. A similar phenomenon was also found across the interface between two solids, which has been termed the “Kapitza thermal resistance” [13]. In randomly dispersed particulate nanocomposites, the Kapitza thermal resistance greatly decreases the effective thermal conductivity with increasing particle size [14–16]. Some analytical and numerical models have been developed to predict the effective thermal conductivity of nanocomposites considering the Kapitza thermal resistance [17–20]. However, for nano-FGMs, these models do not consider the graded microstructure, and thus, a novel model is needed for the accurate design and evaluation of nano-FGMs. This is the emphasis of the present paper.

Yin et al. [8] developed an analytical solution for the heat flux field for the case of a single particle embedded in an FGM matrix.

In that solution, a perfect interface is assumed to exist between particles and the matrix, i.e., with temperature continuity across the interface. Therefore, the interfacial thermal resistance is not considered. This work addresses the effect of the Kapitza thermal resistance on the effective thermal properties of nano-FGMs. A particle with the Kapitza thermal resistance is simulated by a particle with a perfect interface, that is, one having a continuous temperature field across the interface, but modeled with a different thermal conductivity to accommodate the so-called Kapitza effect. Although the local heat flow in the particle with a perfect interface is different from that which would exist in one exhibiting Kapitza thermal resistance, the thermal conductivity of the particle is properly chosen to make the average heat flux of the particle equivalent for the two cases. Using the solution for an equivalent particle embedded in a graded matrix, a self-consistent formulation is developed to derive the average heat flux field of the particle phase. Then, the temperature gradient can be obtained in the gradation direction. From the relation between the effective flux and temperature gradient in the gradation direction, the effective thermal conductivity distribution is obtained.

If the gradient of the volume fraction distribution is zero, the FGM is reduced to a composite containing uniformly dispersed particles. Moreover, by disregarding the Kapitza thermal resistance, the proposed model recovers the conventional self-consistent model for uniform composites [21–23]. Mathematically, effective thermal conductivity is a quantity exactly analogous to effective electric conductivity, dielectric permittivity, magnetic permeability, and water permeability in a linear static state, and thus the solution presented herein can be applied to predict these other effective physical properties of graded materials.

The remainder of this paper is organized as follows. Section 2 presents a self-consistent formulation to determine the effective thermal conductivity distribution for an FGM containing nanoparticles and a continuous matrix. To address the effect of the interface between nanoparticles and the matrix, Sec. 3 proposes a scheme to replace particles with the Kapitza interfacial thermal resistance by an equivalent particle with a perfect interface but a lower thermal conductivity. Section 4 introduces the solution for a single inhomogeneity embedded in an FGM matrix under uniform heat flux field in the gradation direction. Using this solution in the self-consistent formulation, we can analytically obtain effective

¹Corresponding author.

Contributed by the Applied Mechanics Division of ASME for publication in the JOURNAL OF APPLIED MECHANICS. Manuscript received September 24, 2007; final manuscript received April 17, 2008; published online July 24, 2008. Review conducted by Robert M. McMeeking.

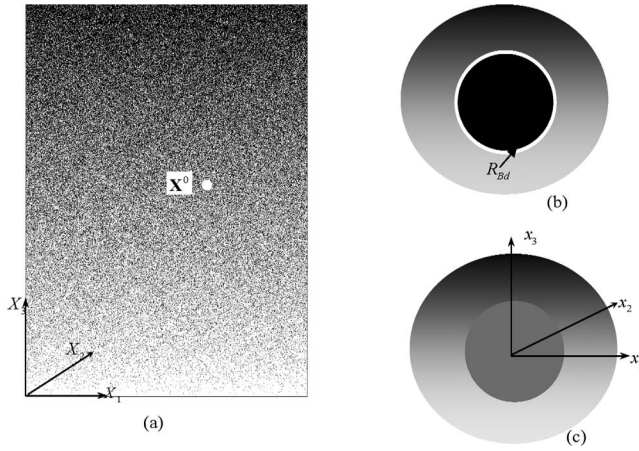


Fig. 1 Illustration of a self-consistent model for FGMs: (a) FGM containing nanoparticles (black) dispersed in Phase B matrix (white), (b) Phase A particle embedded in the FGM itself with an interfacial thermal resistance, and (c) equivalent particle embedded in the FGM with a perfect interface and a lower thermal conductivity

thermal conductivity distribution in the FGM. Section 5 illustrates typical results obtained with the new solution and demonstrates the capability of the proposed model using parametric analyses and comparison with available experimental data.

2 Self-Consistent Formulation

Consider an FGM containing Phase A nanoparticles embedded in a Phase B matrix as shown in Fig. 1(a), where the global coordinate system $X_1-X_2-X_3$ has its origin at the bottom left side of the displayed FGM. The effective thermal conductivity can be tested through the relation between the average heat flux and temperature gradient. A uniform heat flux load q^∞ is applied in the gradation direction. For any material point \mathbf{X}^0 , because the material is homogeneous at each X_1-X_2 layer under steady conditions and without the presence of heat sources, the average heat flux should be equal to q^∞ . At the microscopic scale, both the average heat flux and temperature gradient consist of the two portions from Phases A and B [17]:

$$\langle q_i \rangle^D(X_3^0) = q^\infty \delta_{i3} = \phi(X_3^0) \langle q_i \rangle^A(X_3^0) + [1 - \phi(X_3^0)] \langle q_i \rangle^B(X_3^0) \quad (1)$$

and

$$\langle H_i \rangle^D(X_3^0) = \phi(X_3^0) [\langle H_i \rangle^A(X_3^0) + J_i(X_3^0)] + [1 - \phi(X_3^0)] \langle H_i \rangle^B(X_3^0) \quad (2)$$

where the angle brackets with superscripts D , A , and B denote the volume averages over the whole material point, Phase A, and Phase B, respectively; q_i and H_i represent the heat flux and temperature gradient, respectively, and ϕ is the volume fraction of Phase A. Notice that because the normal component of the heat flux across the interface between the particle and matrix is continuous, the average heat flux only includes two terms from the two material phases; whereas due to a temperature discontinuity existing across the interface, an additional term J_i is introduced to represent the contribution of the temperature jump across the interface, shown schematically in Fig. 1(b) as a white ring. Although shown schematically with finite thickness, the actual interface thickness is infinitesimally small.

The temperature jump is proportional to the normal heat flux across the interface q^n as follows:

$$\Delta T = -R_{Bd} q^n \quad (3)$$

where R_{Bd} denotes the interfacial thermal resistance [14], i.e., the Kapitza thermal resistance. To solve the average heat flux field in

particle Phase A, the self-consistent method [21,22] is used as outlined below.

- For a given point \mathbf{X}^0 in the global FGM system as seen in Fig. 1(a), we build up a local coordinate system with a particle centered at the origin as seen in Fig. 1(c). The thermal conductivity of the graded matrix is assumed to be the same as the FGM itself at the global system.
- Because the particle is in contact with the continuous matrix Phase B, a constant interfacial thermal resistance exists along the interface between the particle and the matrix as seen in Fig. 1(b).
- To solve for the particle's average field, the particle with interfacial thermal resistance is replaced with an equivalent particle with a perfect thermal interface as seen in Fig. 1(c). Therefore, the particle's average heat flux field is obtained from the solution for one particle embedded in an unbounded graded matrix under uniform heat flux at far field.

Through the above procedure, Eq. (2) becomes

$$\langle H_i \rangle^D(X_3^0) = \phi(X_3^0) [\overline{\langle H_i \rangle^A}(X_3^0)] + [1 - \phi(X_3^0)] \langle H_i \rangle^B(X_3^0) \quad (4)$$

where the superscript $\overline{\langle H_i \rangle}$ denotes the presence of a temperature gradient over the equivalent particle. Because the relation between $\langle q_i \rangle^B(X_3^0)$ and $\langle H_i \rangle^B(X_3^0)$ satisfies the Fourier law, if $\langle q_i \rangle^A(X_3^0)$ and $\overline{\langle H_i \rangle^A}(X_3^0)$ can be solved, one can find the relation between overall average heat flux and temperature gradient at point \mathbf{X}^0 . Because \mathbf{X}^0 is arbitrary and can move to any point in the global coordinate system, we can obtain the effective thermal conductivity distribution. Section 3 presents the relation between $\langle q_i \rangle^A(X_3^0)$ and $\overline{\langle H_i \rangle^A}(X_3^0)$, and then Sec. 4 provides the relation between $\langle q_i \rangle^A(X_3^0)$ and the applied test loading q^∞ .

3 Equivalent Particle to Simulate the ‘‘Kapitza Thermal Resistance’’

Although the heat flux field for a particle Ω embedded in an FGM with Kapitza thermal resistance (Fig. 1(b)) is fairly complex, we can treat the particle as a homogeneous particle with a perfect interface as long as the average heat flux and temperature gradient in the new particle are equal to those in the original particle with interfacial thermal resistance. For a stable heat flow in the original particle, observed from the outside surface, the average heat flux field can be written as

$$\langle q_i \rangle_\Omega = \frac{1}{V_\Omega} \left[\int_\Omega q_i(\mathbf{x}) d\mathbf{x} + \int_{\partial\Omega} x_i \Delta q_j(\mathbf{x}) n_j dS \right] \quad (5)$$

where Δq_j denotes the difference of heat flux field cross the interface, and n_j the outward unit normal vector. Based on the continuity of heat flow, we have $\Delta q_j(\mathbf{x}) n_j = 0$ across the interface. Therefore, Eq. (5) is reduced to

$$\langle q_i \rangle_\Omega = \frac{1}{V_\Omega} \int_\Omega q_i(\mathbf{x}) d\mathbf{x} \quad (6)$$

Considering the temperature discontinuity, we can write the average temperature gradient observed from the outside surface as

$$\langle H_i \rangle_\Omega = \frac{1}{V_\Omega} \left[\int_\Omega H_i(\mathbf{x}) d\mathbf{x} + \int_{\partial\Omega} \Delta T(\mathbf{x}) n_i dS \right] \quad (7)$$

Substituting Eq. (3) into the second term on the right hand side of Eq. (7) provides

$$\int_{\partial\Omega} \Delta T(\mathbf{x}) n_i dS = - \int_{\partial\Omega} R_{Bd} (q_j(\mathbf{x}) n_j) n_i dS \quad (8)$$

Because $q_{jj}(\mathbf{x}) = 0$ and $\int_\Omega n_i n_j(\mathbf{x}) d\mathbf{x} = (4/3)\pi a^2 \delta_{ij}$ with a being the radius of the particle, the above equation can be rewritten as

$$\int_{\partial\Omega} \Delta T(\mathbf{x})n_i dS = -\frac{4}{3}\pi a^2 R_{Bd} \langle q_i \rangle_{\Omega} \quad (9)$$

Substituting Eq. (9) into Eq. (7) and using the Fourier law with Eq. (6), we can rewrite Eq. (7) as

$$\langle H_i \rangle_{\Omega} = -\left(\frac{1}{k^A} + \frac{R_{Bd}}{a}\right) \langle q_i \rangle_{\Omega} \quad (10)$$

where k^A denotes the thermal conductivity of the Phase A particle. Therefore, regardless of how complex the local heat flux field is in the particle domain, from an observation point outside the particle, the particle with the Kapitza thermal resistance in Fig. 1(b) is equivalent to a new particle with a perfect interface in Fig. 1(c) but with a lower thermal conductivity, namely, \tilde{k}^A , or,

$$\tilde{k}^A = k^A / (1 + R_{Bd} k^A / a) \quad (11)$$

Therefore, by using Eq. (11) and the Fourier law for Phase B, Eq. (4) can be further rewritten as

$$\langle H_i \rangle^D(X_3^0) = -\phi(X_3^0) \frac{\langle q_i \rangle^A(X_3^0)}{\tilde{k}^A} - [1 - \phi(X_3^0)] \frac{\langle q_i \rangle^B(X_3^0)}{k^B} \quad (12)$$

Combining Eqs. (1) and (12), we can obtain the relation between average heat flux and average temperature gradient if the relation between the particle's average heat flux $\langle q_i \rangle^A(X_3^0)$ and the applied heat flux q^∞ is provided.

4 Single Inhomogeneity in a Functionally Graded Material

A single particle embedded in a homogeneous matrix is a fundamental problem in materials modeling. Eshelby [24,25] derived the elastic solution for an ellipsoidal inclusion embedded in an unbounded matrix with a uniform, far-field loading. Hatta and Taya [26] extended Eshelby's method to heat conduction problems. Yin et al. [8] investigated the heat flux field for a single particle embedded in an FGM matrix.

Consider an unbounded FGM domain with heat conductivity, $k(x_3)$, containing a single spherical inhomogeneity Ω (see Fig. 2) with heat conductivity k^A , radius a , with its center located at the origin. A uniform heat flux field q^∞ is applied in the x_3 direction in the far field. Because the FGM is homogeneous in the x_1 - x_2 plane, if the particle did not exist, then the heat flux field would be uniform. However, a disturbance in the heat flux field q'_i will be induced by the presence of the particle. Then, the local heat flux field can be denoted by two parts:

$$q_i(\mathbf{x}) = q^\infty \delta_{i3} + q'_i(\mathbf{x}) \quad (13)$$

The variation of the FGM properties is assumed to be continuous and differentiable in the gradation direction, so that the thermal conductivity distribution can be written as

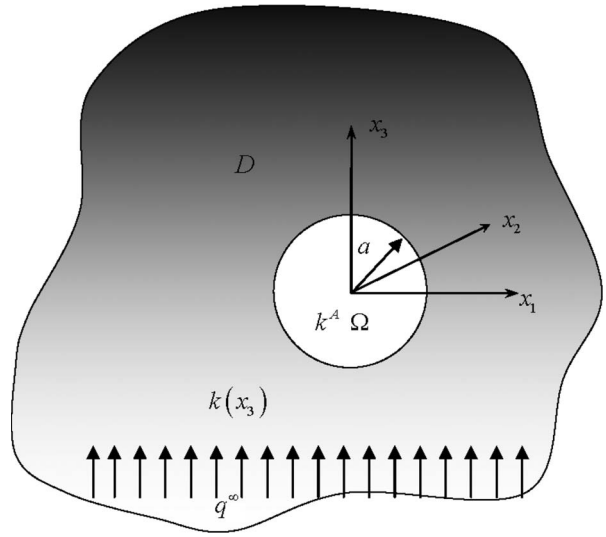


Fig. 2 A single spherical inhomogeneity in an FGM matrix subjected to a uniform heat flux field

$$k(x_3) = k^0(1 + \alpha x_3)^2 + O(x_3^2) \quad (14)$$

where the material variation parameter α is defined as

$$\alpha = 0.5k'(0)/k^0 \quad (15)$$

in which k^0 and $k'(0)$ are the thermal conductivity and its first derivative at the origin, respectively. The higher order terms $O(x_3^2)$ in Eq. (14) will be disregarded for the convenience of derivation. It is noted that accuracy of approximation in Eq. (14) also depends on the magnitude of the material gradient. Yin et al. [8] found that, when $\alpha a \ll 1$, which is satisfied for many FGMs, Eq. (14) provides a high degree of accuracy.

Using Eshelby's equivalent inclusion method, a linearly distributed prescribed heat flux field is introduced in the particle to represent the material mismatch between the particle and the surrounding graded material. The Green's function technique is employed to derive the disturbed heat flux field in Eq. (13). Finally, the heat flux field in both the particle and the graded material can be explicitly written as follows [8]:

$$q_i(\mathbf{x}) = q^\infty \delta_{i3} + q^*(\mathbf{x}) \delta_{3i} - k^0(1 + \alpha x_3) U_{,i}(\mathbf{x}) + k^0 \alpha \delta_{i3} U(\mathbf{x}) \quad (16)$$

where

$$q^*(\mathbf{x}) = \begin{cases} 0, & \mathbf{x} \notin \Omega \\ q^0 + \tilde{q}x_3, & \mathbf{x} \in \Omega \end{cases} \quad (17)$$

$$U(\mathbf{x}) = \begin{cases} \frac{1}{15k^0} [5\rho a q^0 (\rho n_3 - 5\alpha a) - \rho^3 a^2 (1 - 3n_3^2) (\tilde{q} - \alpha q^0) - \alpha \rho^2 a^3 n_3 (\tilde{q} - 2\alpha q^0)], & \mathbf{x} \notin \Omega \\ \frac{1}{30k^0} [q^0 (10x_3 - 5\alpha(3a^2 - |\mathbf{x}|^2)) - (\tilde{q} - \alpha q^0) (5a^2 - 3|\mathbf{x}|^2 - 6x_3^2) - \alpha (\tilde{q} - 2\alpha q^0) (5a^2 - 3|\mathbf{x}|^2) x_3], & \mathbf{x} \in \Omega \end{cases} \quad (18)$$

$$U_{,i}(\mathbf{x}) = \begin{cases} \frac{1}{15k^0} [5q^0 \rho^2 (\rho (\delta_{i3} - 3n_3 n_i) + \alpha n_i) + 3(\tilde{q} - \alpha q^0) \rho^4 a (2\delta_{i3} n_3 + n_i - 5n_3^2 n_i) - \alpha (\tilde{q} - 2\alpha q^0) \rho^3 a^2 (\delta_{i3} - 3n_3 n_i)], & \mathbf{x} \notin \Omega \\ \frac{1}{30k^0} (10q^0 (\delta_{i3} + \alpha x_i) + 6(\tilde{q} - \alpha q^0) (2\delta_{i3} x_3 + x_i) - \alpha (\tilde{q} - 2\alpha q^0) [(5a^2 - 3|\mathbf{x}|^2) \delta_{i3} - 6x_3 x_i]), & \mathbf{x} \in \Omega \end{cases} \quad (19)$$

in which $\mathbf{n}=\mathbf{x}/|\mathbf{x}|$, and $\rho=a/|\mathbf{x}|$, $\alpha=0.5k'(0)/k^0$, and q^0 and \bar{q} are written as

$$q^0 = \frac{k^A - k^0}{3k^A - 2(1 - a^2\alpha^2)(k^A - k^0)} 3q^\infty$$

$$\bar{q} = \frac{2(k^A - k^0)^2 - 15k^0k^A}{(3k^A + 2k^0)[3k^A - 2(1 - a^2\alpha^2)(k^A - k^0)]} 2\alpha q^\infty \quad (20)$$

Taking a volume average of the heat flux field on the particle domain provides the particle's average heat flux as

$$\langle q_i \rangle_\Omega = \frac{3k^A}{3k^A - 2(1 - a^2\alpha^2)[k^A - k^0]} q^\infty \delta_{i3} \quad (21)$$

In Fig. 1(c), the equivalent particle with thermal conductivity \tilde{k}^A is embedded in the FGM with effective thermal conductivity distribution $\bar{k}(X_3)$, which is yet unknown. Using the above equation, we can write the particle's average heat flux as

$$\langle q_i \rangle^A(X_3^0) = \frac{3\tilde{k}^A}{3\tilde{k}^A - 2[1 - a^2\alpha^2(X_3^0)][\tilde{k}^A - k(X_3^0)]} q^\infty \delta_{i3} \quad (22)$$

Using Eqs. (1), (12), and (22), we can derive the relation between the average heat flux and temperature gradient as

$$\langle q_3 \rangle^D(X_3^0) = -k^B \left[1 - \phi(X_3^0) \frac{3(\tilde{k}^A - k^B)}{3\tilde{k}^A - 2[1 - a^2\alpha^2(X_3^0)][\tilde{k}^A - \bar{k}(X_3^0)]} \right]^{-1} \times \langle H_3 \rangle^D(X_3^0) \quad (23)$$

Considering the arbitrariness of choosing \mathbf{X}^0 , we can obtain the effective thermal conductivity at any location as

$$\bar{k}(X_3) = k^B \left[1 - \phi(X_3) \frac{3(\tilde{k}^A - k^B)}{3\tilde{k}^A - 2[1 - a^2\alpha^2(X_3)][\tilde{k}^A - \bar{k}(X_3)]} \right]^{-1} \quad (24)$$

Notice that the above expression is implicit because the right hand side includes $\bar{k}(X_3)$ itself and $\bar{\alpha}$ is still unknown as

$$\bar{\alpha}(X_3) = \frac{1}{2\bar{k}(X_3)} \frac{d\bar{k}(X_3)}{dX_3} \quad (25)$$

We solve Eq. (24) using a recursive method, in which a boundary condition is typically implied as

$$\bar{k}(0) = k^B \quad (26)$$

because the volume fraction of the particle Phase A is zero. For instances where the particle volume fraction does not start from 0%, the modified boundary condition of $\bar{k}(0)$ can be still obtained with the aid of the uniform composite model as seen in Eq. (27).

5 Results and Discussion

For a functionally graded particulate nanocomposite, if the volume fraction of nanoparticles continuously varies in the gradation direction, the effective thermal conductivity distribution can be predicted by Eq. (24) with Eqs. (11), (25), and (26). If the material gradation is zero, the nano-FGM is reduced into a uniformly dispersed nanocomposite, so in Eq. (24) $\bar{\alpha}(X_3)=0$ and the effective thermal conductivity can be rewritten as

$$\bar{k} = k^B \left(1 - 3\phi \frac{\tilde{k}^A - k^B}{\tilde{k}^A + 2\bar{k}} \right)^{-1} \quad (27)$$

The above equation can be ultimately simplified into a quadratic equation with two roots. The correct root places \bar{k} between \tilde{k}^A and k^B .

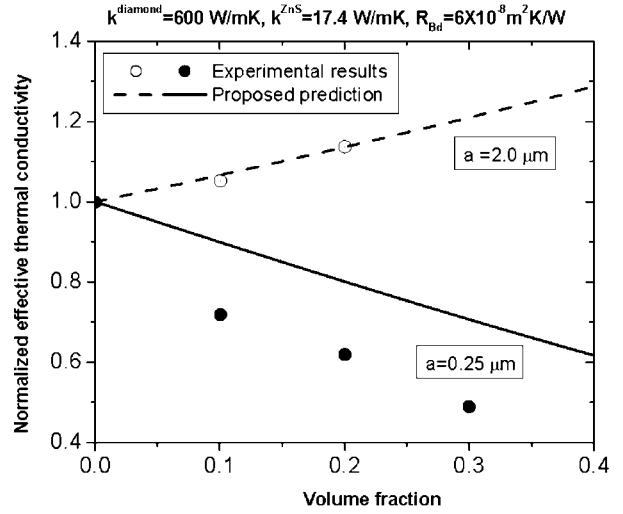


Fig. 3 Effective thermal conductivity versus volume fraction for diamond/ZnS composites

Notice that although this work studies the particle size in nanometers, nanoparticles are still much larger than molecular or atomic scales, so they can be treated as continuous bodies. If the particle's size is fairly large, the effect of the Kapitza thermal resistance can be disregarded, by setting $\tilde{k}^A = k^A$. In this case, the effective thermal conductivity in Eq. (24) can be rewritten as

$$\bar{k}(X_3) = k^B \left[1 - \phi(X_3) \frac{3(k^A - k^B)}{3k^A - 2[1 - a^2\alpha^2(X_3)][k^A - \bar{k}(X_3)]} \right]^{-1} \quad (28)$$

Notice that because $\bar{\alpha}(X_3)$ is related to the volume fraction distribution in its neighborhood, the effective thermal conductivity at a material point not only depends on the volume fraction at the point as shown in Eq. (28), but also depends on the global volume fraction distribution.

Disregarding both the Kapitza thermal resistance and material gradation, the proposed model recovers the conventional self-consistent model as

$$\bar{k} = k^B \left(1 - 3\phi \frac{k^A - k^B}{k^A + 2\bar{k}} \right)^{-1} \quad (29)$$

To demonstrate the capability of the proposed model, we first compare it with available experiments. Every et al. [14] tested the effective thermal conductivity for diamond/ZnS composites with two radii, i.e., $a=250$ nm and 2.0 μm . The other material constants are $k^{\text{diamond}}=600$ W/m K, $k^{\text{ZnS}}=17.4$ W/m K, and $R_{Bd}=6 \times 10^{-8}$ m² K/W. In Fig. 3, for the case of $a=2.0$ μm , the effective thermal conductivity increases with the volume fraction of the diamond particles due to the reinforcement of the particles with much higher thermal conductivity; whereas for the case of $a=250$ nm, the effective thermal conductivity decreases because the interfacial thermal resistance plays a dominant role at this size. The present model predicts the tendency of the experimental data well, although some difference is found for the case of $a=250$ nm due to the irregular particle shape and nonuniform size of particles.

Figure 4 shows the effect of particle size on the effective thermal conductivity distribution in FGMs with linear volume fraction distribution. Here the thickness of the FGMs is set as $H=1$ mm. Four particle sizes are illustrated. For $a=10$ μm , the effective thermal conductivity increases with the volume fraction due to the high thermal conductivity of particles, whereas for $a=10$ nm and 100 nm, the effective thermal conductivity decreases with the vol-

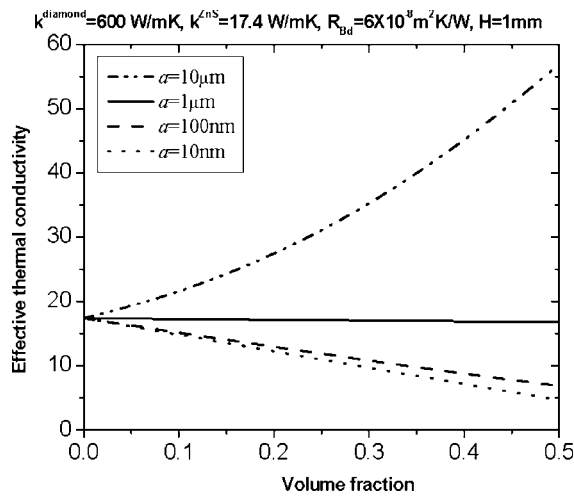


Fig. 4 Predicted effective thermal conductivity versus volume fraction for diamond/ZnS FGMs with different particle sizes

ume fraction due to the Kapitza thermal resistance of nanoparticles. When $a = 1 \mu\text{m}$, the change of thermal conductivity of particles with the volume fraction is quite small because the equivalent thermal conductivity of particles at this size, $\tilde{k}^A = 16.2 \text{ W/mK}$, is fairly close to the thermal conductivity of the matrix, $\tilde{k}^{\text{ZnS}} = 17.4 \text{ W/mK}$. Therefore, the particle size has a dramatic effect on the effective thermal conductivity distribution in FGMs.

To investigate the effect of the Kapitza thermal resistance, Fig. 5 illustrates the effective thermal conductivity distribution of FGMs containing carbon (C) particles and silicon carbide (SiC) matrix assuming different Kapitza thermal resistances. The material constants used are $k^{\text{C}} = 135 \text{ W/mK}$ and $k^{\text{SiC}} = 9.5 \text{ W/mK}$. The volume fraction of carbon particles with radius $a = 1 \mu\text{m}$ varies linearly from 0% to 50% in the gradation direction. The thickness of the FGM is set as $H = 1 \text{ mm}$. With an increase of the Kapitza thermal resistance, the effective thermal resistance decreases considerably. Although the carbon particles have a much higher thermal conductivity than the silicon carbide matrix, the

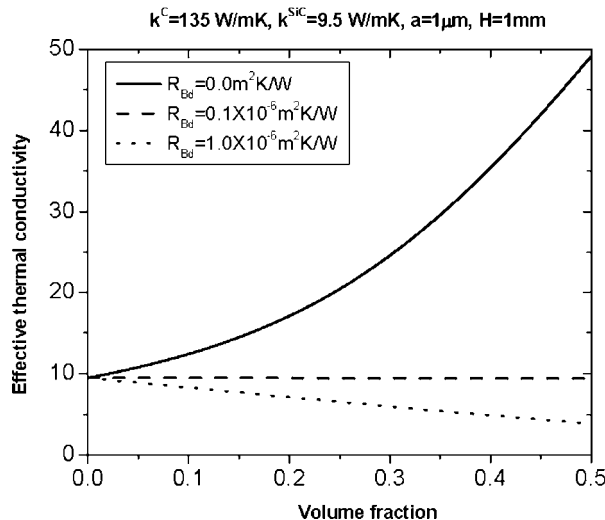


Fig. 5 Predicted effective thermal conductivity versus volume fraction for C/SiC FGMs with different "Kapitza thermal resistances"

particles may not result in an increased effective thermal conductivity if the particle size is fairly low and the Kapitza thermal resistance is considerably high.

Based on the work presented herein, the effective thermal conductivity at a material point in nano-FGMs not only depends on the thermal properties and volume fraction of each phase, which is predicted by conventional composite models, but also considerably depends on the particle size, the Kapitza thermal resistance of the interface, and the material gradient.

6 Conclusions

This work investigates the effective thermal conductivity distribution in nano-FGMs. The "Kapitza thermal resistance" of a nanoparticle is simulated by an equivalent particle with a lower thermal conductivity. A novel self-consistent formulation is developed to derive the average heat flux field of the particle phase based on the analytical solution for a single particle embedded in an FGM matrix. From the relation between the effective flux and temperature gradient in the gradation direction, the effective thermal conductivity distribution is derived.

If the Kapitza thermal resistance is disregarded, the proposed model can also predict the effective thermal conductivity for traditional FGMs. Because effective thermal conductivity is mathematically analogous to effective electric conductivity, dielectric permittivity, magnetic permeability, and water permeability in a linear static state, the solutions developed herein can be extended to obtain these other effective physical properties in graded materials.

If the gradient of the volume fraction distribution is zero, the nano-FGMs are reduced to composites containing uniformly dispersed nanoparticles. An explicit solution of the effective thermal conductivity is provided. Disregarding the interfacial thermal resistance, the proposed model recovers the conventional self-consistent model.

Acknowledgment

This work was sponsored by Federal Highway Administration—National Pooled Fund Study 776, whose support is gratefully acknowledged.

References

- [1] Erdogan, F., Wu, B. H., 1996, "Crack Problems in FGM Layers Under Thermal Stresses," *J. Therm. Stresses*, **19**(3), pp. 237–265.
- [2] Miyamoto, Y., Kaysser, W. A., Rabin, B. H., Kawasaki, A., and Ford, R. G., 1999, *Functionally Graded Materials: Design, Processing and Applications*, Kluwer, Dordrecht.
- [3] Paulino, G. H., Jin, Z. H., and Dodds, R. H., 2003, "Failure of Functionally Graded Materials," *Comprehensive Structural Integrity*, Vol. 2, Elsevier Science, Amsterdam, pp. 607–644.
- [4] Yildirim, B., and Erdogan, F., 2004, "Edge Crack Problems in Homogenous and Functionally Graded Material Thermal Barrier Coatings Under Uniform Thermal Loading," *J. Therm. Stresses*, **27**(4), pp. 311–329.
- [5] Yin, H. M., Sun, L. Z., and Paulino, G. H., 2004, "Micromechanics-Based Elastic Modeling for Functionally Graded Materials With Particle Interactions," *Acta Mater.*, **52**, pp. 3535–3543.
- [6] Yin, H. M., Paulino, G. H., Buttlar, W. G., and Sun, L. Z., 2005, "Effective Thermal Conductivity of Functionally Graded Particulate Composites," *J. Appl. Phys.*, **98**, p. 063704.
- [7] Yin, H. M., Paulino, G. H., Buttlar, W. G., and Sun, L. Z., 2007, "Micromechanics-Based Thermoelastic Model for Functionally Graded Particulate Materials With Particle Interactions," *J. Mech. Phys. Solids*, **55**, pp. 132–160.
- [8] Yin, H. M., Paulino, G. H., Buttlar, W. G., and Sun, L. Z., 2008, "Heat Flux Field for One Spherical Inhomogeneity Embedded in a Functionally Graded Material Matrix," *Int. J. Heat Mass Transfer*, **51**(11–12), pp. 3018–3024.
- [9] Pompea, W., Worch, H., Epple, M., Friess, W., Gelsinsky, M., Greil, P., Hempfle, U., Scharnweber, D., and Schulte, K., 2003, "Functionally Graded Materials for Biomedical Applications," *Mater. Sci. Eng., A*, **362**, pp. 40–60.
- [10] Songa, H. S., Hyuna, S. H., Moona, J., and Song, R. H., 2005, "Electrochemical and Microstructural Characterization of Polymeric Resin-Derived Multilayered Composite Cathode for SOFC," *J. Power Sources*, **145**, pp. 272–277.
- [11] Zhang, Q. J., Tang, X. F., Zhai, P. C., Niino, M., and Endo, C., 2005, "Recent Development in Nano and Graded Thermoelectric Materials," *Mater. Sci. Forum*, **492–493**, pp. 135–140.
- [12] Kapitza, P. L., 1941, "The Study of Heat Transfer in Helium II," *J. Phys.*

- (USSR), **4**, pp. 181–210.
- [13] Swartz, E. T., and Pohl, R. O., 1989, “Thermal-Boundary Resistance,” *Rev. Mod. Phys.*, **61**, pp. 605–668.
- [14] Every, A. G., Tzou, Y., Hasselman, D. P. H., and Raj, R., 1992, “The Effect of Particle Size on the Thermal Conductivity of ZnS/diamond Composites,” *Acta Metall. Mater.*, **40**, pp. 123–129.
- [15] Yang, H.-S., Bai, G.-R., Thompson, L. J., and Eastman, J. A., 2002, “Interfacial Thermal Resistance in Nanocrystalline Yttria-Stabilized Zirconia,” *Acta Mater.*, **50**, pp. 2309–2317.
- [16] Cahill, D. G., Ford, W. K., Goodson, K. E., Mahan, G. D., Majumdar, A., Maris, H. J., Merlin, R., and Phillpot, S. R., 2003, “Nanoscale Thermal Transport,” *J. Appl. Phys.*, **93**, pp. 793–818.
- [17] Benveniste, Y., 1987, “Effective Thermal Conductivity of Composites With a Thermal Contact Resistance Between the Constituents: Nondilute Case,” *J. Appl. Phys.*, **61**, pp. 2840–2843.
- [18] Hasselman, D. P. H. and Johnson, L. F., 1987, “Effective Thermal-Conductivity of Composites With Interfacial Thermal Barrier Resistance,” *J. Compos. Mater.*, **21**, pp. 508–515.
- [19] Nan, C. W., Birringer, R., Clarke, D. R., and Gleiter, H., 1997, “Effective Thermal Conductivity of Particulate Composites With Interfacial Thermal Resistance,” *J. Appl. Phys.*, **81**, pp. 6692–6699.
- [20] Duong, H. M., Papavassiliou, D. V., Lee, L. L., and Mullen, K. J., 2005, “Random Walks in Nanotube Composites: Improved Algorithms and the Role of Thermal Boundary Resistance,” *Appl. Phys. Lett.*, **87**, p. 013101.
- [21] Budiansky, B., 1965, “On the Elastic Moduli of Some Heterogeneous Materials,” *J. Mech. Phys. Solids*, **13**, pp. 223–227.
- [22] Hill, R., 1965, “A Self-Consistent Mechanics of Composite Materials,” *J. Mech. Phys. Solids*, **13**, 213–222.
- [23] Reiter, T., and Dvorak, G. J., 1998, “Micromechanical Models for Graded Composite Materials: II. Thermomechanical Loading,” *J. Mech. Phys. Solids*, **46**, pp. 1655–1673.
- [24] Eshelby, J. D., 1957, “The Determination of the Elastic Field of an Ellipsoidal Inclusion, and Related Problems,” *Proc. R. Soc. London, Ser. A*, **241**, pp. 376–396.
- [25] Eshelby, J. D., 1959, “The Elastic Field Outside an Ellipsoidal Inclusion,” *Proc. R. Soc. London, Ser. A*, **252**, pp. 561–569.
- [26] Hatta, H., and Taya, M., 1986, “Equivalent Inclusion Method for Steady State Heat Conduction in Composites,” *Int. J. Eng. Sci.*, **24**(7), pp. 1159–1172.